Journal of Inorganic Biochemistry 191 (2019) 85–93

Contents lists available at ScienceDirect

Journal of Inorganic Biochemistry

journal homepage: www.elsevier.com/locate/jinorgbio

# Metal-mediated base pairing in DNA involving the artificial nucleobase imidazole-4-carboxylate

Nikolas Sandmann, Denise Defayay, Alexander Hepp, Jens Müller*

*Westfälische Wilhelms-Universität Münster, Institut für Anorganische und Analytische Chemie, Corrensstraße 28/30, 48149 Münster, Germany*

ARTICLE INFO

*Keywords:*
DNA
Imidazole
Metal-mediated base pair
Silver
Copper

ABSTRACT

The use of imidazole-4-carboxylate (**X**) as an artificial nucleobase in metal-mediated base pairing is reported. Towards this end, the corresponding deoxyribonucleoside was synthesized and structurally characterized as its sodium salt (sodium 1,2-dideoxy-1-(4-carboxyimidazol-1-yl)-D-ribofuranose). The deoxyribonucleoside was incorporated into different DNA duplexes (parallel-stranded and antiparallel-stranded), and their Cu(II)- and Ag(I)-binding behavior was investigated. It was shown that both **X**–Cu(II)–**X** and **X**–Ag(I)–**X** base pairs can be formed, with the former being more stabilizing than the latter. The formation of an **X**–Cu(II)–**X** base pair is accompanied by an increase in the duplex melting temperature of approximately 20 °C for antiparallel-stranded duplexes and of 12 °C for the parallel-stranded duplex under investigation. Imidazole-4-carboxylate represents the first imidazole-based nucleoside for Cu(II)-mediated base pairing. Moreover, it is the smallest nucleoside known to form stable Cu(II)-mediated base pairs. Structures of the **X**–Cu(II)–**X** and **X**–Ag(I)–**X** base pairs are proposed, too, based on molecular structures obtained using the model nucleobase 1-benzyl-1*H*-imidazole-4-carboxylate.

## 1. Introduction

The formation of stable nucleic acid duplexes is inevitably dependent on the presence of cations to stabilize the anionic sugar phosphate backbone via electrostatic interactions. In biological systems, alkaline and earth alkaline metal ions regularly serve this purpose [1]. In addition, nucleobases can also bind transition metal ions in a site-specific manner. One of the best-established systems in this respect is the T–Hg(II)–T base pair (T, thymine), in which a mercury(II) ion cross-links two deprotonated thymine residues from opposite strands [2–4]. Similarly, a C:C mispair (C, cytosine) is known to accommodate one Ag(I) ion to form a C–Ag(I)–C base pair [5]. In fact, DNA duplexes can be created that comprise Ag(I)-mediated base pairs only [6–10]. The site-specific incorporation of metal ions into nucleic acid structures has opened an entire new field of applied bioinorganic chemistry [11]. Such conjugates of self-assembling nucleic acids and functionality-bearing metal ions have already been applied in numerous contexts, including the detection of single-nucleotide polymorphisms [12–14], the modification of the charge-transfer properties of DNA [15–20], the generation of DNA-templated metal nanoclusters [21], and more [22]. Interestingly, several reports also indicate that metal-mediated base pairs can be introduced into nucleic acids enzymatically [23–27].

The scope of metal-mediated base pairing has been significantly extended by the introduction of artificial metal-binding nucleosides into the nucleic acids [28,29]. In addition to Ag(I) and Hg(II) ions mentioned above, this also allowed the use of Cu(I) [30], Cu(II) [31–34], Ni(II) [35,36], Zn(II) [37], Pd(II) [38], Mn(III) [39], and others, in metal-mediated base pairs. Even unusual DNA topologies such as three-way junctions, quadruplexes, and other higher-order structures can be stabilized by suitably designed metal-binding nucleic acid components [40–42]. Yet most artificial metal-mediated base pairs appear to include Ag(I) [9,10,43–46]. One of the best investigated Ag(I)-mediated base pairs involves imidazole as artificial nucleobase [47–50]. In addition, a variety of synthetic nucleobases for metal-mediated base pairing have been derived from imidazole, e.g. by attaching alkyl groups to modify the basicity of the ligand [51] or by adding a second binding site and hence generating a bidentate ligand [52].

In this paper, we report for the first time the development of an imidazole-based artificial nucleoside for Cu(II)-mediated base pairing. An inspection of previously reported Cu(II)-mediated base pairs has shown that the most stable ones comprise two identical nucleobases, each one of which contains one neutral and one anionic donor atom. The neutral atom can be oxygen [31] or nitrogen [16,39,53,54], whereas the anionic one persistently is oxygen. In line with these considerations and to ensure an appropriate bite angle of the intended

* Corresponding author.
*E-mail address:* mueller.j@uni-muenster.de (J. Müller).

https://doi.org/10.1016/j.jinorgbio.2018.10.013
Received 31 August 2018; Received in revised form 18 October 2018; Accepted 29 October 2018
Available online 06 November 2018
0162-0134/ 

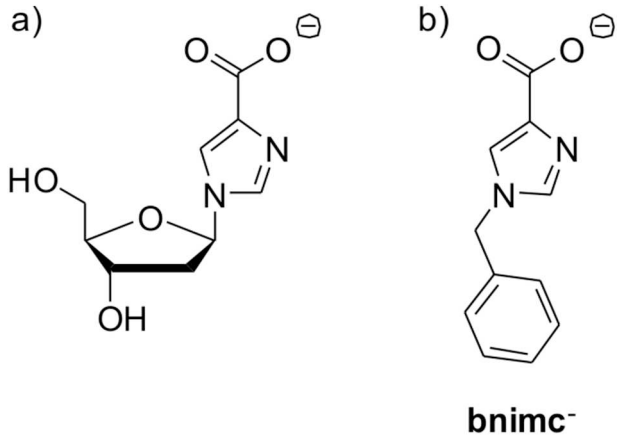


**Chart 1.** Chemical structure of a) the artificial nucleoside under investigation and b) the corresponding model nucleobase.

imidazole-based bidentate ligand, we chose to investigate imidazole-4-carboxylate as a ligand for metal-mediated base pairing (Chart 1a).

## 2. Experimental

1-Benzyl-4-iodoimidazole and Hoffer's chloro sugar were synthesized according to literature procedures [55,56]. Single-crystal X-ray diffraction data were collected with graphite-monochromated Mo Kα radiation (λ = 0.71073 Å) on a Bruker D8 Venture diffractometer. The structures were solved by direct methods and were refined by full-matrix, least squares on $F^2$ by using the SHELXTL and SHELXL-97 programs [57]. Crystallographic data are listed in Table 1. Oligonucleotides were synthesized as reported previously [58]. The oligonucleotides were deprotected and cleaved from the solid support by incubation in 0.1 M NaOH at 55 °C for 14 h. They were purified by denaturing PAGE [gel solution: 7 M urea, 1 TBE buffer, 18% or 14% (depending on the length of the oligonucleotides) polyacrylamide/bisacrylamide (29:1); loading buffer: 11.8 M urea, 42 mM Tris-HCl (pH 7.5), 0.83 mM EDTA (pH 8.0), 8% sucrose] and desalted with NAP 10 columns. Afterwards, they were additionally incubated in 0.1 M NaOH at 55 °C for 14 h, neutralized with 2 M aqueous triethylammonium acetate buffer (pH 7.0) and desalted with NAP 10 columns. The desalted oligonucleotides were characterized by MALDI-ToF mass spectrometry using a 3-hydroxypicolinic acid/ammonium citrate matrix (Figs. S1–S10, Supplementary data). For quantification of the oligonucleotides, a molar extinction coefficient $\varepsilon_{260}$ of 0.04 $M^{-1}$ $cm^{-1}$ was used for $\mathbf{10}^-$. $^1H$ and $^{13}C$ NMR spectra were recorded on Bruker Avance(I) 400 and Avance(III) 400 instruments at 300 K. NMR spectra were referenced to residual solvent peaks (DMSO-$d_6$, $CD_3OD$, $CD_2Cl_2$), to tetramethylsilane ($CDCl_3$) or to 3-(trimethylsilyl)propionate ($D_2O$). HRMS ESI spectra were recorded on an Orbitrap LTQ XXL (Nanospray) from Thermo Scientific. UV and CD (circular dichroism) spectra were recorded using aqueous solutions comprising 1 μM oligonucleotide duplex, 150 mM $NaClO_4$ (except for duplexes **IV** and **IVr**, where 500 mM were used) and 5 mM buffer (2-(cyclohexylamino)ethanesulfonic acid (CHES) at pH 9.0 for the measurements with $Cu(NO_3)_2$ and 3-(*N*-morpholino)propanesulfonic acid (MOPS) at pH 6.8 for the measurements with $AgNO_3$). UV spectra were recorded on a Cary100 Bio instrument between 5 and 75 °C at 1 °C $min^{-1}$. In the UV melting profiles, the absorbance at 260 nm was normalized according to $A_{norm} = (A - A_{min}) / (A_{max} - A_{min})$. Melting temperatures ($T_m$) were determined by applying a Gauss fit to the first derivative of the respective melting profile. CD spectra were recorded at 5 °C on a JASCO J-815 instrument followed by smoothing and manual baseline correction.

### 2.1. Synthesis of methyl 1-benzyl-1H-imidazole-4-carboxylate (4)

Isopropylmagnesium chloride (2 M in THF, 2.25 mL, 4.50 mmol, 1.1 equiv.) was added dropwise to a solution of 1-benzyl-4-iodo-1*H*-imidazole (**3**) (1.16 g, 4.08 mmol, 1.0 equiv.) in dry THF (30 mL). After stirring at ambient temperature for 0.5 h, gaseous $CO_2$ was bubbled through the solution for 5 min. The solid obtained by removing the solvent was dissolved in methanol (50 mL). After cautious addition of thionyl chloride (1.04 mL, 14.3 mmol, 3.5 equiv.), the solution was refluxed for 48 h. The solution was cooled to ambient temperature, the solvent was removed in vacuo, and the residue was dissolved in water (20 mL). After neutralization with aqueous NaOH (1 M), the aqueous layer was extracted with ethyl acetate (3 × 100 mL) and the combined organic layers were dried ($MgSO_4$). After purification by column chromatography ($SiO_2$, ethyl acetate), compound **4** was isolated as a

**Table 1**
Crystallographic data for [Cu(**bnimc**)$_2$($CH_3OH$)$_2$], [$Ag_4$(**bnimc**)$_4$]·4 $H_2O$, compound **7** and Na(**10**).

| | [Cu(**bnimc**)$_2$($CH_3OH$)$_2$] | [$Ag_4$(**bnimc**)$_4$]·4 $H_2O$ | **7** | Na(**10**) |
|---|---|---|---|---|
| Empirical formula | $C_{24}H_{26}CuN_4O_6$ | $C_{22}H_{22}Ag_2N_4O_6$ | $C_{20}H_{28}N_4O_{10}$ | $C_9H_{11}N_2NaO_5$ |
| Formula weight | 530.03 | 654.17 | 484.46 | 250.19 |
| Crystal system | Triclinic | Monoclinic | Orthorhombic | Orthorhombic |
| Space group | *P*–1 | $P2_1/c$ | $P2_12_12_1$ | $P2_12_12_1$ |
| *a*/Å | 5.2023(12) | 7.7354(5) | 5.16500(10) | 5.6142(5) |
| *b*/Å | 10.525(3) | 23.0010(15) | 10.0259(2) | 9.2098(8) |
| *c*/Å | 11.995(4) | 12.7547(8) | 43.0366(8) | 20.0500(16) |
| *α*/° | 110.268(14) | 90 | 90 | 90 |
| *β*/° | 93.096(12) | 93.639(2) | 90 | 90 |
| γ/° | 103.517(8) | 90 | 90 | 90 |
| *V*/Å$^3$ | 592.4(3) | 2264.8(3) | 2228.60(7) | 1036.70(15) |
| *Z* | 1 | 4 | 4 | 4 |
| $\rho_{calcd.}$/g $cm^{-1}$ | 1.49 | 1.92 | 1.60 | 1.44 |
| $\mu$(Mo-$K_\alpha$)/$mm^{-1}$ | 1.0 | 1.8 | 1.0 | 0.2 |
| Crystal size/mm | 0.24 × 0.09 × 0.02 | 0.63 × 0.06 × 0.06 | 0.16 × 0.14 × 0.02 | 0.24 × 0.06 × 0.03 |
| Temperature/K | 100(2) | 100(2) | 100(2) | 100(2) |
| $\theta_{min}$, $\theta_{max}$/° | 2.25, 27.85 | 2.39, 30.10 | 4.11, 76.51 | 2.43, 27.94 |
| Dataset | −6:6, −13:13, −15:15 | −10:10, −32:32, −17:18 | −6:6, −12:11, −52:53 | −7:7, −12:12, −26:26 |
| Tot., uniq. Data | 6846, 2765 | 32,065, 6637 | 15,192, 4483 | 14,305, 2488 |
| Observed data [$I > 2\sigma(I)$] | 2395 | 4952 | 4268 | 2336 |
| $N_{ref}$, $N_{par}$ | 2765, 162 | 6637, 323 | 4483, 313 | 2488, 159 |
| Flack parameter | n/a | n/a | 0.04(6) | 0.03(13) |
| *R*, $wR_2$, *S* [$I > 2\sigma(I)$] | 0.0387, 0.1200, 0.897 | 0.0347, 0.0713, 1.012 | 0.0317, 0.0915, 0.735 | 0.0301, 0.0692, 1.089 |
| Resd. dens. min. and max./e Å$^{-3}$ | 0.474, −0.327 | 0.824, −0.591 | 0.193, −0.291 | 0.254, −0.228 |

white solid (565 mg, 2.61 mmol, 64%). HRMS ESI *m/z*: $[M + Na]^+$ 239.0787 (calcd. 239.0796). Elemental analysis (%): found: C 66.5, H 5.3, N 13.1; calcd. for $C_{12}H_{12}N_2O_2$: C 66.7, H 5.6, N 13.0. $^1$H NMR (400 MHz, DMSO-$d_6$), *δ*/ppm: 7.96 (d, 1.3 Hz, 1H, H2), 7.89 (d, 1.3 Hz, 1H, H5), 7.41–7.23 (m, 5H, benzyl), 5.24 (s, 2H, $CH_2$), 3.72 (s, 3H, $CH_3$). $^{13}$C NMR (101 MHz, DMSO-$d_6$), *δ*/ppm: 162.5 (C═O), 138.7 (C2), 136.9 (C4), 132.2 (benzyl, *ipso*), 128.7 (benzyl, *meta*), 127.9 (benzyl, *para*), 127.9 (benzyl, *ortho*), 126.2 (C5), 50.8 ($CH_3$), 49.8 ($CH_2$).

### 2.2. Synthesis of sodium 1-benzyl-1H-imidazole-4-carboxylate (Na(**5**))

A solution of **4** (450 mg, 2.08 mmol, 1.0 equiv.) in aqueous NaOH (0.1 M, 22.9 mL, 1.1 equiv.) was stirred for 12 h at 55 °C. After removal of the solvent in vacuo, the product was recrystallized from ethanol to yield the sodium salt of $\mathbf{5}^-$ as colorless crystals (466 mg, 2.08 mmol, 100%). HRMS ESI *m/z*: $[M + H]^+$ 225.0634 (calcd. 225.0640). Elemental analysis (%): found: C 58.8, H 3.8, N 12.3; calcd. for $C_{11}H_9N_2NaO_2$: C 58.9, H 4.1, N 12.5. $^1$H NMR (400 MHz, $D_2O$, pD 7.7), *δ*/ppm: 7.67 (d, 1.5 Hz, 1H, H2), 7.54 (d, 1.5 Hz, 1H, H5), 7.43–7.33 (m, 3H, benzyl), 7.27 (dd, 7.7 Hz, 1.8 Hz, 2H, benzyl), 5.16 (s, 2H, $CH_2$). $^{13}$C NMR (101 MHz, $D_2O$, pD 7.7), *δ*/ppm: 168.3 (C═O), 135.9 (C2), 135.6 (C4), 134.1 (benzyl, *ipso*), 126.7 (benzyl, *meta*), 126.0 (benzyl, *para*), 125.3 (benzyl, *ortho*), 121.6 (C5), 48.3 ($CH_2$).

### 2.3. Synthesis of the Cu(II) complex [Cu(**bnimc**)$_2$($CH_3OH$)$_2$]

An aqueous solution (1 mL) of $Cu(OAc)_2{\cdot}H_2O$ (22 mg, 0.11 mmol, 0.5 equiv.) was added to an aqueous solution (10 mL) of ligand Na(**5**) (50 mg, 0.22 mmol, 1.0 equiv.). After 0.5 h, the blue precipitate was filtered, washed with water (10 mL), ethanol (5 mL) and diethylether (10 mL) and dried (56 mg, 0.11 mmol, 50%). Single crystals of [Cu(**bnimc**)$_2$($CH_3OH$)$_2$] (**bnimc**$^-$ = 1-benzyl-1*H*-imidazole-4-carboxylate) suitable for X-ray diffraction analysis were obtained by vapor diffusion crystallization in methanol with diethylether as antisolvent. HRMS ESI *m/z*: $[M + Na]^+$ 488.0515 (calcd. 488.0522). Elemental analysis (%): found: C 54.0, H 4.4, N 11.5; calcd. for $C_{22}H_{18}CuN_4O_4{\cdot}1.5\ H_2O$: C 53.6, H 4.3, N 11.4.

### 2.4. Synthesis of the Ag(I) complex [Ag$_4$(**bnimc**)$_4$]·4 $H_2O$

An aqueous solution (1 mL) of $AgClO_4$ (50 mg, 0.22 mmol, 1.0 equiv.) was added to an aqueous solution (10 mL) of ligand Na(**5**) (50 mg, 0.22 mmol, 1.0 equiv.). The colorless precipitate was filtered, washed with water (10 mL), ethanol (5 mL) and diethylether (10 mL) and dried (35 mg, 0.10 mmol, 45%). Single crystals suitable for X-ray diffraction analysis were obtained by vapor diffusion crystallization in acetonitrile with diethylether as antisolvent. HRMS ESI *m/z*: [Ag(**bnimc**)$_2$]$^-$ 509.0349 (calcd. 509.0379). Elemental analysis (%): found: C 37.4, H 2.5, N 8.0; calcd. for $C_{11}H_9AgN_2O_2{\cdot}2.5\ H_2O$: C 37.3, H 4.0, N 7.9. $^1$H NMR (400 MHz, $CDCl_3$), *δ*/ppm: 8.08 (s, 1H, H2), 7.67 (s, 1H, H5), 7.40–7.27 (m, 5H, benzyl), 5.26 (s, 2H, $CH_2$). $^{13}$C NMR (101 MHz, $CDCl_3$), *δ*/ppm: 165.5 (C═O), 138.2 (C2), 137.1 (benzyl), 136.4 (C4), 128.7 (benzyl), 128.0 (benzyl), 127.7 (benzyl), 122.5 (C4), 50.3 ($CH_2$).

### 2.5. Synthesis of 3,5-di-O-p-toluoyl-1,2-dideoxy-1-(4-(methylcarboxy) imidazol-1-yl)-D-ribofuranose (**6**)

Methyl 1*H*-imidazole-4-carboxylate (500 mg, 3.96 mmol, 1.0 equiv.) was suspended in dry THF (30 mL). Sodium hydride (60% in mineral oil, 238 mg, 5.95 mmol, 1.5 equiv.) was added at 0 °C. After 0.5 h of stirring, Hoffer's chloro sugar (2.29 g, 5.95 mmol, 1.5 equiv.) was added in three portions over 1 h. The reaction mixture was stirred at ambient temperature overnight, and the solvent was removed in vacuo. The residue was dissolved in $CH_2Cl_2$ (100 mL) and washed with water (3 × 25 mL). The organic layer was dried ($MgSO_4$) and the solvent removed in vacuo. After purification by column chromatography (cyclohexane:ethyl acetate 2:1 → ethyl acetate), compound **6** was obtained as a white solid (965 mg, 2.02 mmol, 51%). HRMS ESI *m/z*: $[M + Na]^+$ 501.1649 (calcd. 501.1638). Elemental analysis (%): found: C 65.1, H 5.4, N 5.8; calcd. for $C_{26}H_{26}N_2O_7$: C 65.3, H 5.5, N 5.9. $^1$H NMR (400 MHz, $CDCl_3$), *δ*/ppm: 7.94–7.90 (m, 2H, Tol), 7.89–7.85 (m, 2H, Tol), 7.76 (d, 1.4 Hz, 1H, H5), 7.70 (d, 1.4 Hz, 1H, H2), 7.28–7.21 (m, 4H, Tol), 6.13 (dd, 8.1 Hz, 5.6 Hz, 1H, H1′), 5.65 (dt, 6.1 Hz, 2.4 Hz, 1H, H3′), 4.62 (d, 3.7 Hz, 2H, H5′, H5″), 4.58 (td, 3.7 Hz, 2.4 Hz, 1H, H4′), 3.83 (s, 3H, $OCH_3$), 2.75 (ddd, 14.2 Hz, 5.7 Hz, 2.4 Hz, 1H, H2′), 2.64 (ddd, 14.2 Hz, 8.1 Hz, 6.2 Hz, 1H, H2″), 2.42 (s, 3H, $CH_3$), 2.40 (s, 3H, $CH_3$). $^{13}$C NMR (101 MHz, $CDCl_3$), *δ*/ppm: 166.1 (C═O (Tol)), 165.8 (C═O (Tol)), 162.8 (C═O), 144.6 (Tol), 144.2 (Tol), 136.2 (C2), 134.4 (C4), 129.7 (Tol), 129.6 (Tol), 129.3 (Tol), 129.3 (Tol), 126.5 (Tol), 126.2 (Tol), 122.5 (C5), 86.6 (C1′), 83.1 (C4′), 74.8 (C3′), 63.8 (C5′), 51.6 ($OCH_3$), 39.6 (C2′), 21.7 ($CH_3$), 21.6 ($CH_3$).

### 2.6. Synthesis of 1,2-dideoxy-1-(4-(methylcarboxy)-1H-imidazol-1-yl)-D-ribofuranose (**7**)

Compound **6** (1.14 g, 2.37 mmol, 1.0 equiv.) was suspended in a solution of sodium methoxide (282 mg, 5.22 mmol, 2.2 equiv.) in methanol (30 mL) and stirred at ambient temperature for 2 h. The solvent was removed in vacuo. After purification of the residue by column chromatography ($CH_2Cl_2$:methanol 10:1), compound **7** was obtained as an off-white solid (466 mg, 1.92 mmol, 81%). This compound was structurally characterized by single crystal X-ray diffraction analysis (Fig. S11, Supplementary data). HRMS ESI *m/z*: $[M + H]^+$ 243.0989 (calcd. 243.0981). Elemental analysis (%): found: C 49.5, H 6.0, N 11.6; calcd. for $C_{10}H_{14}N_2O_5$: C 49.6, H 5.8, N 11.6. $^1$H NMR (400 MHz, $CD_3OD$), *δ*/ppm: 8.08 (d, 1.4 Hz, 1H, H5), 8.02 (d, 1.4 Hz, 1H, H2), 6.16 (t, 6.5 Hz, 1H, H1′), 4.50 (dt, 5.6 Hz, 3.8 Hz, 1H, H3′), 4.02 (q, 3.8 Hz, 1H, H4′), 3.88 (s, 3H, $OCH_3$), 3.81–3.69 (m, 2H, H5′, H5″), 2.55–2.44 (m, 2H, H2′, H2″). $^{13}$C NMR (101 MHz, $CD_3OD$), *δ*/ppm: 164.4 (C═O), 138.7 (C2), 134.1 (C4), 124.9 (C5), 89.4 (C4′), 88.2 (C1′), 72.4 (C3′), 63.0 (C5′), 52.1 ($OCH_3$), 42.9 (C2′).

### 2.7. Synthesis of 5-O-(4,4′-dimethoxytrityl)-1,2-dideoxy-1-(4-(methylcarboxy)-1H-imidazol-1-yl)-D-ribofuranose (**8**)

4,4′-Dimethoxytrityl chloride (787 mg, 2.33 mmol, 1.2 equiv.) was added to a solution of compound **7** (466 mg, 1.94 mmol, 1.0 equiv.) in dry pyridine (20 mL) in the presence of catalytic amounts of 4′-(dimethylamino)pyridine and stirred at ambient temperature for 2 h. The solution was diluted with $CH_2Cl_2$ (50 mL) and washed with saturated aqueous $NaHCO_3$ (3 × 20 mL). The organic layer was dried ($MgSO_4$) and the solvent removed in vacuo. After purification by column chromatography (cyclohexane:ethyl acetate:triethylamine 2:1:0.03 → ethyl acetate:methanol:triethylamine 1:0.05:0.03), compound **8** was obtained as a white foam (943 mg, 1.70 mmol, 88%). HRMS ESI *m/z*: $[M + Na]^+$ 567.2140 (calcd. 567.2107). Elemental analysis (%): found: C 67.5, H 6.1, N 4.9; calcd. for $C_{31}H_{32}N_2O_7{\cdot}0.5\ H_2O$: C 67.3, H 6.0, N 5.1. $^1$H NMR (400 MHz, $CD_2Cl_2$), *δ*/ppm: 7.74 (d, 1.4 Hz, 1H, H5), 7.62 (d, 1.3 Hz, 1H, H2), 7.43–7.38 (m, 2H, DMT), 7.32–7.25 (m, 6H, DMT), 7.24–7.18 (m, 1H, DMT), 6.85 – 6.80 (m, 4H, DMT), 6.03 (t, 6.4 Hz, 1H, H1′), 4.56 (dt, 5.9 Hz, 3.6 Hz, 1H, H3′), 4.16–4.06 (m, 1H, H4′), 3.77 (s, 9H, $OCH_3$), 3.33 (dd, 10.3 Hz, 4.8 Hz, 1H, H5′ or H5″), 3.24 (dd, 10.3 Hz, 4.2 Hz, 1H, H5′ or H5″), 2.52–2.37 (m, 2H, H2′, H2″). $^{13}$C NMR (101 MHz, $CD_2Cl_2$), *δ*/ppm: 163.3 (C═O), 159.1 (DMT), 145.2 (DMT), 137.0 (C2), 136.1 (DMT), 136.0 (DMT), 134.2 (C4), 130.4 (DMT), 128.4 (DMT), 128.3 (DMT), 127.2 (DMT), 123.4 (C5), 113.6 (DMT), 86.9 (C1′), 86.8 (C4′), 72.4 (C3′), 64.3 (C5′), 55.6 ($OCH_3$ (DMT)), 51.7 ($OCH_3$), 42.2 (C2′).

### 2.8. Synthesis of 2-cyanoethyl (5-O-(4,4′-dimethoxytrityl)-1,2,3-trideoxy-1-(4-(methylcarboxy)-1H-imidazol-1-yl)-D-ribofuranos-3-yl) diisopropylphosphoramidite (9)

*N*,*N*-Diisopropylethylamine (144 µL, 0.827 mmol, 4.6 equiv.) was added to a solution of compound **8** (100 mg, 0.181 mmol, 1.0 equiv.) in dry $CH_2Cl_2$ (2 mL). Cyanoethyl-*N*,*N*-diisopropylchlorophosphoramidite (56 µL, 0.25 mmol, 1.4 equiv.) was added, and the solution was stirred at ambient temperature for 2 h. After purification by column chromatography (cyclohexane:ethyl acetate:triethylamine 1:1:0.01), compound **9** was obtained as a mixture of diastereomers as a white foam (121 mg, 0.162 mmol, 90%). HRMS ESI *m/z*: $[M + Na]^+$ 767.3184 (calcd. 767.3186). $^1$H NMR (400 MHz, $CD_2Cl_2$), *δ*/ppm: 7.82–7.72 (m, 1H, H5), 7.64 (m, 1H, H2), 7.45–7.38 (m, 2H, DMT), 7.35–7.19 (m, 7H, DMT), 6.90–6.78 (m, 4H, DMT), 6.08–5.97 (m, 1H, H1′), 4.68–4.53 (m, 1H, H3′), 4.30–4.16 (m, 1H, H4′), 3.78 (s, 9H, $OCH_3$), 3.75–3.54 (m, 4H, $OCH_2$, CH), 3.34–3.20 (m, 2H, H5′, H5″), 2.67–2.57 (m, 1H, H2′), 2.57–2.52 (m, 1H, H2″), 2.52–2.36 (m, 2H, $CH_2CN$), 1.22–1.05 (m, 12H, $CH_3$). $^{31}$P NMR (162 MHz, $CD_2Cl_2$), *δ*/ppm: 148.9, 148.8.

### 2.9. Synthesis of sodium 1,2-dideoxy-1-(4-carboxyimidazol-1-yl)-D-ribofuranose (Na(10))

A solution of compound **7** (100 mg, 0.413 mmol, 1.0 equiv.) in aqueous NaOH (0.1 M, 41 mL, 1.0 equiv.) was stirred at ambient temperature for 3 d. After removal of the solvent in vacuo, the product was obtained as a white solid (103 mg, 0.412 mmol, 100%). This compound was structurally characterized by single crystal X-ray diffraction analysis (Fig. S12, Supplementary data). HRMS ESI *m/z*: $[M + H]^+$ 251.0638 (calcd. 251.0644). Elemental analysis (%): found: C 38.9, H 4.7, N 10.0; calcd. for $C_9H_1N_2NaO_5{\cdot}1.5\ H_2O$: C 39.0, H 5.1, N 10.1. $^1$H NMR (400 MHz, $D_2O$, pD 7.6), *δ*/ppm: 7.85 (d, 1.3 Hz, 1H, H2), 7.72 (d, 1.4 Hz, 1H, H5), 6.16 (t, 6.5 Hz, 1H, H1′), 4.52 (dt, 5.9 Hz, 3.9 Hz, 1H, H3′), 4.08 (dt, 5.3 Hz, 3.8 Hz, 1H, H4′), 3.77 (dd, 12.3 Hz, 4.0 Hz, 1H, H5′ or H5″), 3.68 (dd, 12.3 Hz, 5.5 Hz, 1H, H5′ or H5″), 2.62–2.43 (m, 2H, H2′, H2″). $^{13}$C NMR (101 MHz, $D_2O$, pD 7.6), *δ*/ppm: 170.4 (C═O), 138.4 (C4), 137.0 (C2), 121.1 (C5), 86.9 (C4′), 86.2 (C1′), 70.9 (C3′), 61.6 (C5′), 39.9 (C2′).

## 3. Results and discussion

### 3.1. Synthesis of model nucleobase and nucleoside

To investigate the applicability of imidazole-4-carboxylate (**imc**$^-$) as a ligand in metal-mediated base pairing, a model nucleobase was synthesized first. In model nucleobases, the carbohydrate moiety is formally replaced by an alkyl group, leaving only the nucleobase donor atoms available for metal ion coordination. Moreover, this approach simplifies the NMR spectra and makes crystallization more likely. Model nucleobases have been prominently used in deciphering the binding mode of cisplatin [59,60], but have also been highly valuable in determining possible geometries of metal-mediated base pairs [39,61–67]. We therefore decided to investigate the coordination chemistry of 1-benzyl-1*H*-imidazole-4-carboxylate (**bnimc**$^-$, Chart 1b). Its synthesis is shown in Scheme 1. Based on literature procedures, 1-benzyl-4-iodoimidazole **3** was obtained from imidazole in a three-step procedure. Initially, imidazole was iodinated to give 4,5-diiodoimidazole **1** [68]. Subsequent deprotonation and alkylation gave 1-benzyl-4,5-diiodo-1*H*-imidazole **2** [55]. Using a Grignard reaction, the 5-iodo substituent was selectively removed to give 1-benzyl-4-iodoimidazole **3** [55]. In a second Grignard reaction with gaseous $CO_2$, the remaining iodo substituent was replaced by a carboxylate group, which was transformed into the respective methyl ester without prior purification, yielding methyl 1-benzyl-1*H*-imidazole-4-carboxylate **4**. Finally saponification quantitatively gave the sodium salt of 1-benzyl-1*H*-imidazole-4-carboxylate (Na(**5**), Na(**bnimc**)) in a clean reaction.

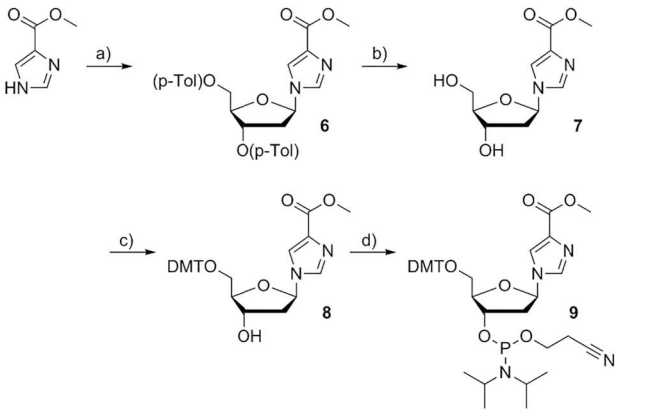


**Scheme 2.** Synthesis of the phosphoramidite **9**. a) 1. NaH, $CH_3CN$, 2. Hoffer's chloro sugar, 51%; b) $NaOCH_3$, $CH_3OH$, 81%; c) DMT-Cl, 4′-(dimethylamino) pyridine, pyridine, 89%; d) *N*,*N*-diisopropylethylamine, CEDIP-Cl, $CH_2Cl_2$, 77%.

To obtain the phosphoramidite required for an automated solid-phase synthesis of oligonucleotides bearing an imidazole-4-carboxylate-containing deoxyribonucleoside, commercially available methyl 1*H*-imidazole-4-carboxylate was deprotonated and reacted with Hoffer's chloro sugar to give the *p*-toluoyl-protected nucleoside **6** (Scheme 2). Removal of the *p*-toluoyl protecting groups gave the free nucleoside **7**, still bearing a methyl group at the carboxylate (as required during solid-phase oligonucleotide synthesis). Consecutive introduction of DMT (4,4′-dimethoxytrityl) and CEDIP (cyanoethyl *N*,*N*-diisopropyl phosphoramidite) protecting groups at the primary and secondary OH groups finally gave the required phosphoramidite **9**. In a separate reaction, the methyl ether **7** was saponified using aqueous NaOH to give the sodium salt of the free nucleoside **10**$^-$.

### 3.2. Metal complexation behavior of the model nucleobase

Various metal complexes of derivatives of imidazole-4-carboxylate (**imc**$^-$) have been reported in the past, including Cu(II) complexes. The Cu(II) complex of 1-methylimidazole-4-carboxylate (**mimc**$^-$) [Cu(**mimc**)$_2$(OH$_2$)$_2$] adopts a distorted octahedral coordination geometry with trans-oriented ligands [69]. When using unsubstituted imidazole-4-carboxylate, a planar complex [Cu(**imc**)$_2$] is obtained, likewise displaying a trans orientation of the ligands [70,71]. Interestingly, complexes involving other metal ions also show ligands in a cis orientation,

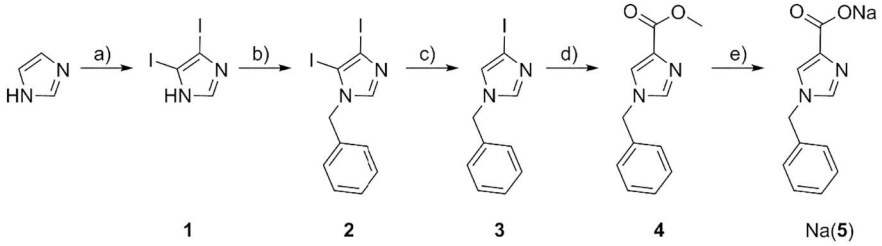


**Scheme 1.** Synthesis of sodium 1-benzyl-1*H*-imidazole-4-carboxylate (Na(**5**)). The first three steps were performed following literature procedures [55,68]. a) NaOH, $I_2$, KI, $H_2O$, 61%; b) 1. NaH, THF, 2. benzyl bromide, 76%; c) 1. isopropyl magnesium chloride, THF, 2. $H_2O$, $NH_4Cl$, 77%; d) 1. isopropyl magnesium chloride, THF, 2. $CO_2$, 3. $CH_3OH$, $SOCl_2$, 64%; e) NaOH, $H_2O$, 100%.

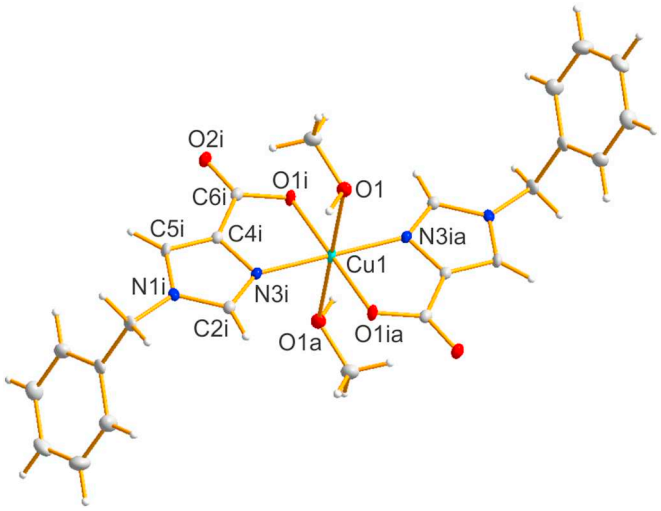


**Fig. 1.** Molecular structure of [Cu(**bnimc**)$_2$(CH$_3$OH)$_2$]. Ellipsoids are drawn at the 50% probability level.

as for example observed in [Zn(**imc**)$_2$(OH$_2$)$_2$] [72]. The ability to form complexes both with cis- and trans-orientation of the ligand is of importance in the context of metal-mediated base pairing in antiparallel- and parallel-stranded DNA (vide infra).

Our studies using the model nucleobase **bnimc**$^-$ confirm the preference of Cu(II) complexes to adopt a trans orientation of the ligands. The complex [Cu(**bnimc**)$_2$(CH$_3$OH)$_2$], obtained by combining aqueous solutions of Na(**5**) and Cu(II) acetate and subsequent recrystallization of the blue precipitate from methanol, contains two axially coordinated methanol ligands in addition to the **bnimc**$^-$ ligands. Fig. 1 shows the molecular structure of [Cu(**bnimc**)$_2$(CH$_3$OH)$_2$], and Table 2 lists representative bond lengths and angles. Assuming a dissociation of the weakly bound methanol ligands, the planar complex of Cu(II) and imidazole-4-carboxylate should be ideally suited for an incorporation as a metal-mediated base pair into an oligonucleotide duplex. In such a base pair, the N1 atoms bonded to the benzyl substituents in the model nucleobase would be involved in the glycosidic bonds. To enable a trans orientation of the N1 atoms as observed in the crystal structure, the use of a parallel-stranded DNA duplex would be advisable, as most parallel-stranded nucleic acid duplexes display a trans orientation of the glycosidic bonds [73].

As numerous metal-mediated base pairs have been reported using Ag(I) ions as central metal ions incorporated into the base pairs, we also investigated the formation of an Ag(I) complex of the model nucleobase **bnimc**$^-$. As would be required for metal-mediated base pair formation, two **bnimc**$^-$ moieties combine with one Ag(I) ion. In the resulting [Ag$_4$(**bnimc**)$_4$] complex, two such [Ag(**bnimc**)$_2$]$^-$ units dimerize via two additional Ag(I) ions. Fig. 2 shows the molecular structure of [Ag$_4$(**bnimc**)$_4$]. Each individual [Ag(**bnimc**)$_2$]$^-$ unit of the tetranuclear complex represents the structure of the anticipated Ag(I)-mediated base pair. One of these units is indicated by a frame in Fig. 2. The N1 atoms are in a cisoid arrangement, which is in agreement with the requirements for an incorporation as a metal-mediated base pair within a B-DNA double helix [74]. Table 3 lists representative

**Table 2**
Selected bond lengths and angles in [Cu(**bnimc**)$_2$(CH$_3$OH)$_2$].

| | Bond length/Å | | Bond angle/° |
|---|---|---|---|
| Cu1–N3i | 1.972(2) | N3i–Cu1–O1i | 83.64(7) |
| Cu1–O1i | 1.969(2) | N3i–Cu1–O1 | 88.66(7) |
| Cu1–O1 | 2.509(2) | O1i–Cu1–O1 | 91.11(6) |

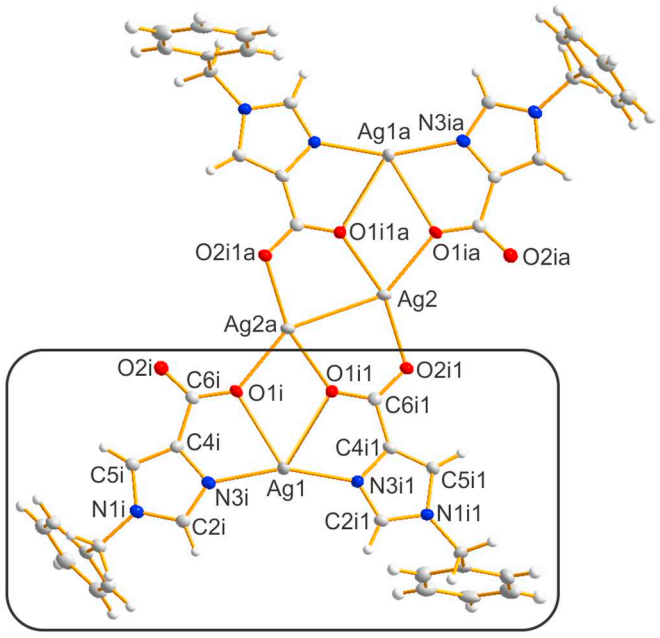


**Fig. 2.** Molecular structure of [Ag$_4$(**bnimc**)$_4$]·4 H$_2$O. Ellipsoids are drawn at the 50% probability level. Water of hydration is not shown. The frame designates the section modeling the anticipated Ag(I)-mediated base pair.

**Table 3**
Selected bond lengths and angles in [Ag$_4$(**bnimc**)$_4$]·4 H$_2$O.

| | Bond length/Å | | Bond angle/° |
|---|---|---|---|
| Ag1–N3i | 2.174(2) | N3i–Ag1–N3i1 | 158.52(9) |
| Ag1–N3i1 | 2.157(2) | N3i–Ag1–O1i | 70.06(8) |
| Ag1–O1i | 2.599(2) | N3i1–Ag1–O1i | 129.56(8) |
| Ag1–O1i1 | 2.746(2) | O2i1–Ag2–O1i1a | 159.62(7) |
| Ag2–O2i1 | 2.193(2) | O1i–Ag2a–Ag2 | 148.03(5) |
| Ag2–Ag2a | 2.9507(5) | | |
| Ag2a–O1i | 2.308(2) | | |
| Ag2a–O1i1 | 2.241(2) | | |

interatomic distances and bond angles. It is interesting to note that the Ag(I) ion is located asymmetrically in-between the two **bnimc**$^-$ ligands, as particularly evident from the two different Ag1−O bond lengths (Ag1–O1i, 2.599(2) Å; Ag1–O1i1, 2.746(2) Å). The latter bond is rather long, but several precedents exist for such long Ag−O distances [75,76]. Moreover, the bond length is well within the sum of the van der Waals radii of the elements involved [77]. In [Ag$_4$(**bnimc**)$_4$], two [Ag(**bnimc**)$_2$]$^-$ entities are bridged via two Ag(I) ions. In the resulting carboxylate-bridged dimer, a short Ag2–Ag2a distance of 2.9507(5) Å is observed, indicating the possibility of argentophilic interactions [78]. In the crystal structure, additional short Ag-Ag contacts are present between [Ag$_4$(**bnimc**)$_4$] moieties of neighboring planes (Ag1–Ag2, 2.9366(5) Å, symmetry operation for Ag2: 1 + *x*, *y*, *z*), leading to the formation of a supramolecular network (not shown).

### 3.3. Characterization of the artificial nucleoside

Prior to any metal complexation study performed in water, the acidity constants of the respective ligand need to be established to rule out a possible competition of protonation and metalation events. Towards this end, the $^1$H NMR chemical shifts of the free nucleoside **10**$^-$ were monitored in a pD-dependent fashion (Fig. 3). A least-squares fit of the data indicates the presence of two p$K_a$ values at 1.95 ± 0.05 and 5.36 ± 0.02 (Table S1, Supplementary data) [79], assigned to the deprotonation of the carboxylic acid and the imidazole moiety,

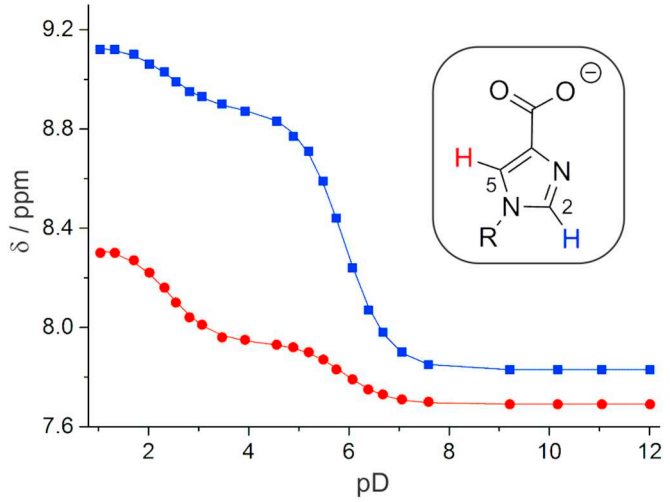


**Fig. 3.** pD-dependent $^{1}$H NMR chemical shifts of H**10**, including least-squares fit assuming two p$K_a$ values (■: H2, ●: H5). The inset shows the structure of **10**$^-$ including an atom numbering scheme of the relevant hydrogen atoms (R = 2′-deoxyribose).

respectively. Hence, the artificial nucleobase is fully deprotonated above ca. pH 6, suggesting that competing protonation events do not take place under neutral and alkaline conditions.

During the preparation of the free nucleoside **10**$^-$ required for the p$K_a$ determination, single crystals of its sodium salt were obtained that were suitable for a structure determination by X-ray diffraction analysis. Fig. 4 shows the molecular structure of **10**$^-$. A structure including the sodium ion is given in the Supplementary data (Fig. S12). The 1,2-dideoxy-1-(4-carboxyimidazol-1-yl)-D-ribofuranose adopts a C3′-*endo* conformation (Table S2, Supplementary data). The artificial nucleobase is oriented anti with respect to the carbohydrate, with the designated metal binding sites N3i and O1i pointing in the direction of the center of a hypothetical double helix. Hence, the structure corroborates the applicability of this artificial nucleoside in metal-mediated base pairing.

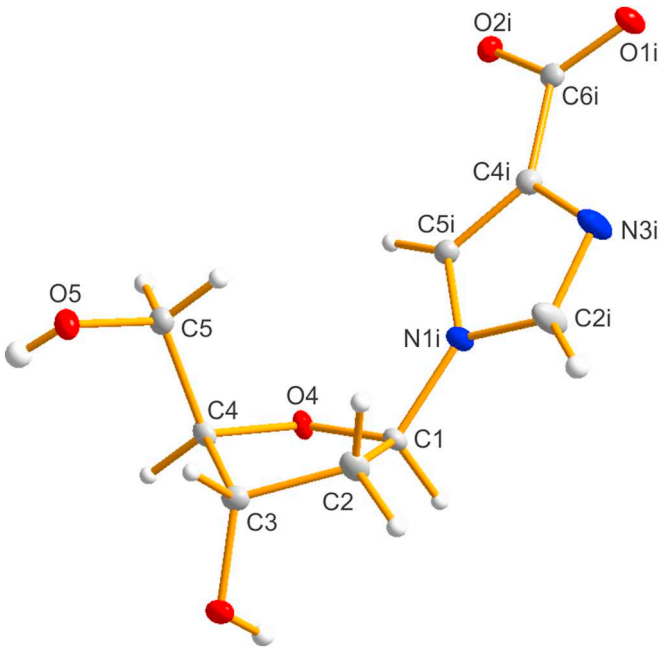


**Fig. 4.** Molecular structure of the anion 1,2-dideoxy-1-(4-carboxyimidazol-1-yl)-D-ribofuranose (**10**$^-$). Ellipsoids are drawn at the 50% probability level.

### 3.4. Formation of metal-mediated base pairs

To investigate the capability of imidazole-4-carboxylate to engage in metal-mediated base pairing, four DNA oligonucleotide duplexes were synthesized and evaluated (Table 4). Duplexes **I–III** contain one **X**:**X** pair each (**X** = 1,2-dideoxy-1-(4-carboxyimidazol-1-yl)-D-ribofuranose), whereas duplex **IV** comprises two **X**:**X** pairs. Moreover, the former duplexes are antiparallel-stranded, whereas a parallel strand arrangement is adopted in the latter case. For comparison, reference duplexes **Ir–IVr** were investigated, too. In these duplexes, the **X**:**X** pairs were formally replaced by G:C (duplexes **Ir** and **IIr**) or A:T (duplexes **IIIr** and **IVr**) base pairs, to make the duplexes devoid of designated metal-binding sites (G, guanine; A, adenine).

The formation of a metal-mediated base pair is typically accompanied by an increase in thermal stability, caused by the formation of coordinate bonds and evident from a rise in the melting temperature $T_m$ [22]. Accordingly, $T_m$ was determined for all duplexes under investigation by means of temperature-dependent UV spectroscopy. The data obtained for duplex **I** will be described in detail in the following, whereas the corresponding data for duplexes **II–IV** and for all reference duplexes are given in the Supplementary data. Fig. 5 shows the melting curves of duplex **I** in the presence of increasing amounts of Cu(II). As can nicely be seen, the initial addition of Cu(II) leads to a large increase in $T_m$. As expected for metal-mediated base pair formation, the addition of more than one Cu(II) per **X**:**X** pair does not influence the thermal stability any further. In case of reference duplex **Ir** without the designated Cu(II)-binding site, no significant change in $T_m$ is observed upon the addition of Cu(II) (Table 5 and Supplementary data, Fig. S13). Hence, it can be concluded that in duplex **I** one Cu(II) binds per **X**:**X** pair to give an **X**–Cu(II)–**X** base pair. The formation of this base pair is accompanied by a significant increase of the melting temperature $T_m$ from 22.0 °C to 41.9 °C ($\Delta T_m$ = 19.9 °C). According to a CD spectroscopic study, the B-DNA conformation of duplex **I** is little affected by the formation of the **X**–Cu(II)–**X** base pair (Supplementary data, Fig. S14a). Similar results were obtained for duplexes **II–IV** and the corresponding reference duplexes (Supplementary data, Figs. S15–S20). Table 5 summarizes the increase in melting temperature upon the formation of **X**–Cu(II)–**X** base pairs for all four duplexes, Chart 2 shows the proposed structure of the metal-mediated base pair.

It is worth highlighting some peculiarities of duplex **IV**, which is the only parallel-stranded duplex among the investigated ones. As a result of its less favored parallel strand orientation, its melting temperature is lower than those of the antiparallel-stranded duplexes. Nonetheless, the incorporation of Cu(II) to form **X**–Cu(II)–**X** base pairs is accompanied by a large increase in thermal stability. In fact, the thermal stability of duplex **IV** after formation of the **X**–Cu(II)–**X** base pairs is essentially identical to that of the reference duplex **IVr**. In other words, the destabilization evoked by the introduction of **X**:**X** mispairs is compensated by their involvement in metal-mediated base pair formation. The thermal stabilization of ca. 11.7 °C per **X**–Cu(II)–**X** base pair is much smaller than that observed for the antiparallel-stranded duplexes **I–III** though. This finding is unexpected, because for geometric considerations duplex **IV** must contain the metal-mediated pairs with a transoid orientation of the glycosidic bonds (Chart 2b) [73]. This orientation was found to be the preferred one outside the DNA context, as evident from the crystal structure of the model nucleobase complex (Fig. 1). Presumably, the transoid **X**–Cu(II)–**X** base pair does not perfectly match the geometry of a parallel-stranded duplex. This assumption is corroborated by the observation of a change in the CD spectrum of duplex **IV** upon the formation of the Cu(II)-mediated base pairs (Supplementary data, Fig. S19b).

As the unsubstituted imidazole nucleobase has been reported as an excellent Ag(I)-binding ligand, we also investigated the applicability of imidazole-4-carboxylate in Ag(I)-mediated base pairing. Again, duplexes **I–IV** were investigated. Fig. 6 shows the melting curves of duplex **I** in the presence of increasing amounts of Ag(I). As had already been

**Table 4**
Oligonucleotide duplexes investigated in this study (**X** = imidazole-4-carboxylic acid).

| | Sequence | Chemical formula | Entry | $[M + H]^+$/Da | |
|---|---|---|---|---|---|
| | | | | Calcd. | Found[a] |
| Duplex **I** | 5′-d(GAG GGT **X**TG AAA G)-3′ | $C_{129}H_{159}N_{56}O_{75}P_{12}$ | ODN1 | 4064 | 4064 |
| | 3′-d(CTC CCA **X**AC TTT C)-5′ | $C_{123}H_{161}N_{38}O_{79}P_{12}$ | ODN2 | 3806 | 3805 |
| Duplex **Ir** | 5′-d(GAG GGT GTG AAA G)-3′ | $C_{130}H_{160}N_{59}O_{74}P_{12}$ | | | [80] |
| | 3′-d(CTC CCA CAC TTT C)-5′ | $C_{123}H_{162}N_{39}O_{78}P_{12}$ | | | |
| Duplex **II** | 5′-d(CAC ATT A**X**T GTT GTA)-3′ | $C_{147}H_{187}N_{50}O_{91}P_{14}$ | ODN3 | 4542 | 4543 |
| | 3′-d(GTG TAA T**X**A CAA CAT)-5′ | $C_{147}H_{185}N_{56}O_{87}P_{14}$ | ODN4 | 4560 | 4561 |
| Duplex **IIr** | 5′-d(CAC ATT AGT GTT GTA)-3′ | $C_{148}H_{188}N_{53}O_{90}P_{14}$ | ODN5 | 4581 | 4581 |
| | 3′-d(GTG TAA TCA CAA CAT)-5′ | $C_{147}H_{186}N_{57}O_{86}P_{14}$ | ODN6 | 4559 | 4559 |
| Duplex **III** | 5′-d(TTT GTT TGT TTG **X**TT GTT TTT TTT TT)-3′ | $C_{259}H_{334}N_{64}O_{176}P_{25}$ | ODN7 | 7930 | 7931 |
| | 3′-d(AAA CAA ACA AAC **X**AA CAA AAA AAA AA)-5′ | $C_{255}H_{313}N_{119}O_{134}P_{25}$ | ODN8 | 7959 | 7962 |
| Duplex **IIIr** | 5′-d(TTT GTT TGT TTG TTT GTT TTT TTT TT)-3′ | | | | [81] |
| | 3′-d(AAA CAA ACA AAC AAA CAA AAA AAA AA)-5′ | | | | |
| Duplex **IV** | 5′-d(AAA AAA AAA **X**TA ATT TT**X** AAT ATT T)-3′ | $C_{248}H_{309}N_{92}O_{145}P_{24}$ | ODN9 | 7638 | 7643 |
| | 5′-d(TTT TTT TTT **X**AT TAA AA**X** TTA TAA A)-3′ | $C_{248}H_{314}N_{77}O_{155}P_{24}$ | ODN10 | 7593 | 7596 |
| Duplex **IVr** | 5′-d(AAA AAA AAA ATA ATT TTA AAT ATT T)-3′ | | | | [37] |
| | 5′-d(TTT TTT TTT TAT TAA AAT TTA TAA A)-3′ | | | | |

[a] The MALDI-ToF mass spectra are given in the Supplementary data (Figs. S1–S10) unless the duplexes have been reported previously.

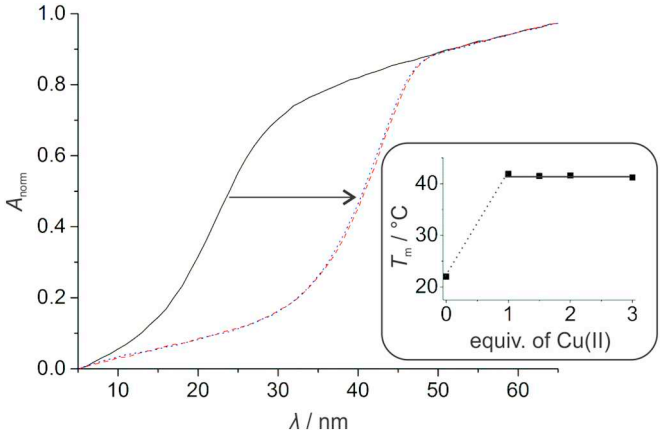


**Fig. 5.** Melting curves of duplex **I** in the presence of various amounts of Cu(II) (solid line: no Cu(II); broken line: one Cu(II); dotted line: two Cu(II)). The inset shows the melting temperature $T_m$ depending on the equivalents of Cu(II) per duplex. Experimental conditions: 1 μM duplex, 150 mM $NaClO_4$, 5 mM CHES (pH 9.0).

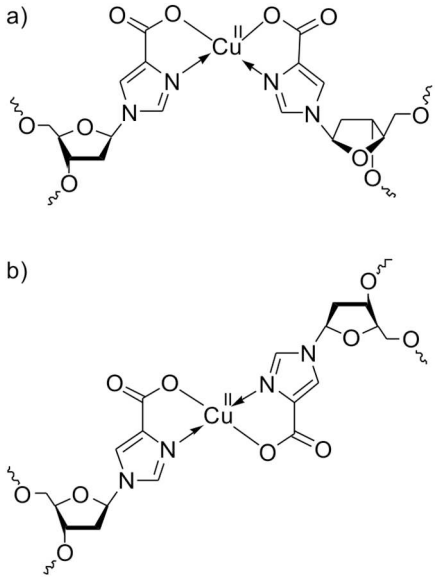


**Chart 2.** Structural representation of the **X**–Cu(II)–**X** base pair in a) antiparallel-stranded and b) parallel-stranded DNA.

**Table 5**
Melting temperature ($T_m$/°C) of all duplexes under investigation prior to and after the addition of one metal ion per **X**:**X** pair. The change in melting temperature ($\Delta T_m$/°C) is given, too.

| Duplex | Cu(II)[a] | | | Ag(I)[b] | | |
|---|---|---|---|---|---|---|
| | $T_m$ (no Cu) | $T_m$ (Cu) | $\Delta T_m$ | $T_m$ (no Ag) | $T_m$ (Ag) | $\Delta T_m$ |
| **I** | 22.0 | 41.9 | 19.9 | 20.2 | 37.6 | 17.4 |
| **Ir** | 50.0 | 50.1 | 0.1 | 51.5 [80] | 52.7 [80] | 1.2 [80] |
| **II** | 24.2 | 43.0 | 18.8 | 24.8 | 40.1 | 15.3 |
| **IIr** | 47.3 | 47.0 | −0.3 | 49.1 | 50.4 | 1.3 |
| **III** | 46.3 | 61.2 | 14.9 | 48.7 | 57.9 | 9.2 |
| **IIIr** | 57.6 | 57.6 | 0.0 | 56.7 [81] | 57.0 [81] | 0.3 [81] |
| **IV** | 14.6 | 38.1 | 23.5 | 16.0 | 37.4 | 21.4 |
| **IVr** | 37.6 | 37.6 | 0.0 | 39.6 | 40.5 | 0.9 |

[a] Data acquired at pH 9.0
[b] Data acquired at pH 6.8.

observed upon the addition of Cu(II), a significant rise in $T_m$ is found when one Ag(I) is added per **X**:**X** pair. The addition of excess Ag(I) does not lead to significant further increase in the melting temperature. According to the CD spectra, the B-DNA conformation is not affected by the presence of Ag(I) (Supplementary data, Fig. S14b). Moreover, Ag(I) does not influence the thermal stability of the reference duplex **Ir** (Supplementary data, Fig. S21). Hence, it can be reasoned that an **X**–Ag(I)–**X** base pair is formed in duplex **I**. The same conclusion can be drawn for duplexes **II**–**IV** (Supplementary data, Figs. S22–S27). As can be seen from a comparison of the melting temperatures of the duplexes in the presence of Ag(I) and Cu(II), respectively, **X**–Cu(II)–**X** are significantly more stabilizing than **X**–Ag(I)–**X** base pairs (Table 5).

## 4. Summary and conclusions

For the first time, an imidazole-based artificial nucleoside has been used to generate a Cu(II)-mediated base pair. By applying imidazole-4-carboxylate (X), highly stabilizing **X**–Cu(II)–**X** base pairs were formed in a variety of different DNA duplexes. Notably, these **X**–Cu(II)–**X** base pairs are compatible with both antiparallel-stranded and parallel-stranded duplexes. In the former case, the formation of such a base pair is accompanied by an increase in duplex melting temperature $T_m$ of approximately 20 °C, whereas $T_m$ increases by only ~12 °C per **X**–Cu(II)–**X** base pair in the latter case. The **X**–Cu(II)–**X** base pairs are more

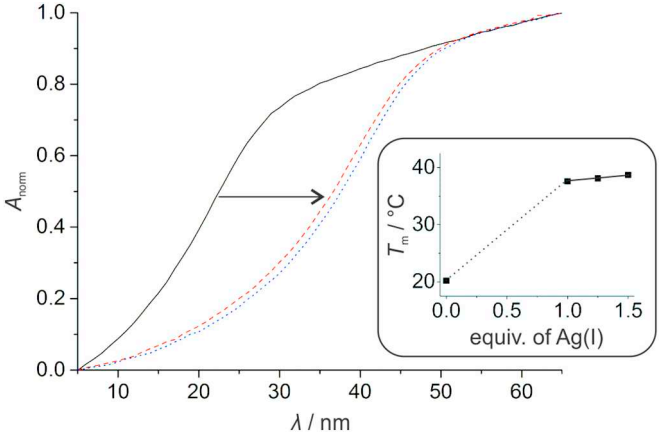


**Fig. 6.** Melting curves of duplex **I** in the presence of various amounts of Ag(I) (solid line: no Ag(I); broken line: one Ag(I); dotted line: two Ag(I)). The inset shows the melting temperature $T_m$ depending on the equivalents of Ag(I) per duplex. Experimental conditions: 1 μM duplex, 150 mM $NaClO_4$, 5 mM MOPS (pH 6.8).

stabilizing than the corresponding **X**–Ag(I)–**X** base pairs in the same duplex sequences. Hence, the design principle of providing one neutral and one anionic donor site to guarantee the formation of an overall neutral **X**–Cu(II)–**X** base pair was applied successfully. Imidazole-4-carboxylate is the smallest Cu(II)-binding nucleobase reported to date. Due to its small aromatic surface, its π stacking interactions with neighboring nucleobases do not significantly contribute to duplex stability, as evident from the low melting temperatures in the absence of Ag(I) or Cu(II) ions. Hence, the large increase in $T_m$ upon the formation **X**–Cu(II)–**X** base pairs can be attributed to the generation of the coordinate bonds. Due to its simplicity, imidazole-4-carboxylate is expected to become a prominent artificial nucleobase for metal-mediated base pairing.

## Abbreviations

| | |
|---|---|
| A | adenine |
| **bnimc**$^-$ | 1-benzyl-1*H*-imidazole-4-carboxylate |
| C | cytosine |
| CD | circular dichroism |
| CEDIP | cyanoethyl *N*,*N*-diisopropyl phosphoramidite |
| CHES | 2-(cyclohexylamino)ethanesulfonic acid |
| DMT | 4,4′-dimethoxytrityl |
| G | guanine |
| **imc**$^-$ | 1*H*-imidazole-4-carboxylate |
| **mimc**$^-$ | 1-methyl-1*H*-imidazole-4-carboxylate |
| MOPS | 3-(*N*-morpholino)propanesulfonic acid |
| T | thymine |
| $T_m$ | melting temperature |
| **X** | imidazole-4-carboxylate |

## Appendix A. Supplementary data

CCDC 1863218-1863221 contain the supplementary crystallographic data for this paper. These data can be obtained free of charge from The Cambridge Crystallographic Data Centre via www.ccdc.cam.ac.uk/data_request/cif. Supplementary data to this article can be found online at doi.10.1016/j.jinorgbio.2018.10.013.

## References

[1] J. Müller, Metallomics 2 (2010) 318–327.
[2] S. Katz, Nature 194 (1962) 569.
[3] Z. Kuklenyik, L.G. Marzilli, Inorg. Chem. 35 (1996) 5654–5662.
[4] H. Yamaguchi, J. Šebera, J. Kondo, S. Oda, T. Komuro, T. Kawamura, T. Dairaku, Y. Kondo, I. Okamoto, A. Ono, J.V. Burda, C. Kojima, V. Sychrovský, Y. Tanaka, Nucleic Acids Res. 42 (2014) 4094–4099.
[5] T. Dairaku, K. Furuita, H. Sato, J. Šebera, K. Nakashima, J. Kondo, D. Yamanaka, Y. Kondo, I. Okamoto, A. Ono, V. Sychrovský, C. Kojima, Y. Tanaka, Chem. Eur. J. 22 (2016) 13028–13031.
[6] J. Kondo, Y. Tada, T. Dairaku, Y. Hattori, H. Saneyoshi, A. Ono, Y. Tanaka, Nat. Chem. 9 (2017) 956–960.
[7] D.A. Megger, C. Fonseca Guerra, J. Hoffmann, B. Brutschy, F.M. Bickelhaupt, J. Müller, Chem. Eur. J. 17 (2011) 6533–6544.
[8] F.-A. Polonius, J. Müller, Angew. Chem. Int. Ed. 46 (2007) 5602–5604.
[9] N. Santamaría-Díaz, J.M. Méndez-Arriaga, J.M. Salas, M.A. Galindo, Angew. Chem. Int. Ed. 55 (2016) 6170–6174.
[10] J.M. Méndez-Arriaga, C.R. Maldonado, J.A. Dobado, M.A. Galindo, Chem. Eur. J. 24 (2018) 4583–4589.
[11] Y. Takezawa, M. Shionoya, J. Müller, J.L. Atwood (Ed.), Comprehensive Supramolecular Chemistry II, vol. 4, Elsevier Ltd., Oxford, 2017, pp. 259–293.
[12] B. Jash, J. Müller, Eur. J. Inorg. Chem. (2017) 3857–3861.
[13] Y.-W. Lin, H.-T. Ho, C.-C. Huang, H.-T. Chang, Nucleic Acids Res. 36 (2008) e123.
[14] H. Torigoe, A. Ono, T. Kozasa, Transit. Met. Chem. 36 (2011) 131–144.
[15] J. Joseph, G.B. Schuster, Org. Lett. 9 (2007) 1843–1846.
[16] T. Ehrenschwender, W. Schmucker, C. Wellner, T. Augenstein, P. Carl, J. Harmer, F. Breher, H.-A. Wagenknecht, Chem. Eur. J. 19 (2013) 12547–12552.
[17] S. Liu, G.H. Clever, Y. Takezawa, M. Kaneko, K. Tanaka, X. Guo, M. Shionoya, Angew. Chem. Int. Ed. 50 (2011) 8886–8890.
[18] S. Hensel, K. Eckey, P. Scharf, N. Megger, U. Karst, J. Müller, Chem. Eur. J. 23 (2017) 10244–10248.
[19] J.C. Léon, Z. She, A. Kamal, M.H. Shamsi, J. Müller, H.-B. Kraatz, Angew. Chem. Int. Ed. 56 (2017) 6098–6102.
[20] E. Toomey, J. Xu, S. Vecchioni, L. Rothschild, S. Wind, G.E. Fernandes, J. Phys. Chem. C 120 (2016) 7804–7809.
[21] J.C. Léon, G. González-Abradelo, C.A. Strassert, J. Müller, Chem. Eur. J. 24 (2018) 8320–8324.
[22] B. Jash, J. Müller, Chem. Eur. J. 23 (2017) 17166–17178.
[23] T. Kobayashi, Y. Takezawa, A. Sakamoto, M. Shionoya, Chem. Commun. 52 (2016) 3762–3765.
[24] T. Funai, J. Nakamura, Y. Miyazaki, R. Kiriu, O. Nakagawa, S.-i. Wada, A. Ono, H. Urata, Angew. Chem. Int. Ed. 53 (2014) 6624–6627.
[25] E.-K. Kim, C. Switzer, ChemBioChem 14 (2013) 2403–2407.
[26] T. Funai, Y. Miyazaki, M. Aotani, E. Yamaguchi, O. Nakagawa, S.-i. Wada, H. Torigoe, A. Ono, H. Urata, Angew. Chem. Int. Ed. 51 (2012) 6464–6466.
[27] C. Kaul, M. Müller, M. Wagner, S. Schneider, T. Carell, Nat. Chem. 3 (2011) 794–800.
[28] Y. Takezawa, J. Müller, M. Shionoya, Chem. Lett. 46 (2017) 622–633.
[29] G.H. Clever, C. Kaul, T. Carell, Angew. Chem. Int. Ed. 46 (2007) 6226–6236.
[30] B. Jash, J. Müller, Angew. Chem. Int. Ed. 57 (2018) 9524–9527.
[31] K. Tanaka, A. Tengeiji, T. Kato, N. Toyama, M. Shionoya, Science 299 (2003) 1212–1213.
[32] K. Tanaka, G.H. Clever, Y. Takezawa, Y. Yamada, C. Kaul, M. Shionoya, T. Carell, Nat. Nanotechnol. 1 (2006) 190–194.
[33] S. Atwell, E. Meggers, G. Spraggon, P.G. Schultz, J. Am. Chem. Soc. 123 (2001) 12364–12367.
[34] H. Weizman, Y. Tor, J. Am. Chem. Soc. 123 (2001) 3375–3376.
[35] C. Switzer, S. Sinha, P.H. Kim, B.D. Heuberger, Angew. Chem. Int. Ed. 44 (2005) 1529–1532.
[36] C. Switzer, D. Shin, Chem. Commun. (2005) 1342–1344.
[37] B. Jash, J. Müller, J. Inorg. Biochem. 186 (2018) 301–306.
[38] S.K. Maity, T. Lönnberg, Chem. Eur. J. 24 (2018) 1274–1277.
[39] G.H. Clever, Y. Söltl, H. Burks, W. Spahl, T. Carell, Chem. Eur. J. 12 (2006) 8708–8718.
[40] Y. Takezawa, S. Yoneda, J.-L.H.A. Duprey, T. Nakama, M. Shionoya, Chem. Sci. 7 (2016) 3006–3010.
[41] D.M. Engelhard, J. Nowack, G.H. Clever, Angew. Chem. Int. Ed. 56 (2017) 11640–11644.
[42] H. Yang, C.K. McLaughlin, F.A. Aldaye, G.D. Hamblin, A.Z. Rys, I. Rouiller, H.F. Sleiman, Nat. Chem. 1 (2009) 390–396.
[43] X. Guo, P. Leonard, S.A. Ingale, J. Liu, H. Mei, M. Sieg, F. Seela, Chem. Eur. J. 24 (2018) 8883–8892.
[44] H. Zhao, P. Leonard, X. Guo, H. Yang, F. Seela, Chem. Eur. J. 23 (2017) 5529–5540.
[45] H. Yang, H. Mei, F. Seela, Chem. Eur. J. 21 (2015) 10207–10219.
[46] N. Zimmermann, E. Meggers, P.G. Schultz, J. Am. Chem. Soc. 124 (2002) 13684–13685.
[47] S. Johannsen, N. Megger, D. Böhme, R.K.O. Sigel, J. Müller, Nat. Chem. 2 (2010) 229–234.
[48] S. Kumbhar, S. Johannsen, R.K.O. Sigel, M.P. Waller, J. Müller, J. Inorg. Biochem. 127 (2013) 203–210.
[49] K. Schweizer, J.C. Léon, B.J. Ravoo, J. Müller, J. Inorg. Biochem. 160 (2016) 256–263.
[50] X. Tan, S. Litau, X. Zhang, J. Müller, Langmuir 31 (2015) 11305–11310.
[51] S. Hensel, N. Megger, K. Schweizer, J. Müller, Beilstein J. Org. Chem. 10 (2014) 2139–2144.
[52] K. Schweizer, J. Kösters, J. Müller, J. Biol. Inorg. Chem. 20 (2015) 895–903.
[53] L. Zhang, E. Meggers, J. Am. Chem. Soc. 127 (2005) 74–75.
[54] M. Su, M. Tomás-Gamasa, S. Serdjukow, P. Mayer, T. Carell, Chem. Commun. 50 (2014) 409–411.
[55] C.J. Lovely, H. Du, R. Sivappa, M.R. Bhandari, Y. He, H.V.R. Dias, J. Organomet.

Chem. 72 (2007) 3741–3749.
[56] V. Rolland, M. Kotera, J. Lhomme, Synth. Commun. 27 (1997) 3505–3511.
[57] G.M. Sheldrick, Acta Cryst A64 (2008) 112–122.
[58] P. Scharf, B. Jash, J.A. Kuriappan, M.P. Waller, J. Müller, Chem. Eur. J. 22 (2016) 295–301.
[59] B. Lippert, G. Raudaschl, C.J.L. Lock, P. Pilon, Inorg. Chim. Acta 93 (1984) 43–50.
[60] H. Schöllhorn, G. Raudaschl-Sieber, G. Müller, U. Thewalt, B. Lippert, J. Am. Chem. Soc. 107 (1985) 5932–5937.
[61] D.A. Megger, J. Kösters, A. Hepp, J. Müller, Eur. J. Inorg. Chem. (2010) 4859–4864.
[62] K. Seubert, D. Böhme, J. Kösters, W.-Z. Shen, E. Freisinger, J. Müller, Z. Anorg. Allg. Chem. 638 (2012) 1761–1767.
[63] C. Radunsky, D.A. Megger, A. Hepp, J. Kösters, E. Freisinger, J. Müller, Z. Anorg. Allg. Chem. 639 (2013) 1621–1627.
[64] I. Sinha, J. Kösters, A. Hepp, J. Müller, Dalton Trans. 42 (2013) 16080–16089.
[65] T. Richters, O. Krug, J. Kösters, A. Hepp, J. Müller, Chem. Eur. J. 20 (2014) 7811–7818.
[66] I. Sinha, A. Hepp, J. Kösters, J. Müller, J. Inorg. Biochem. 153 (2015) 355–360.
[67] S. Mandal, C. Wang, R.K. Prajapati, J. Kösters, S. Verma, L. Chi, J. Müller, Inorg. Chem. 55 (2016) 7041–7050.
[68] C.J. Lovely, H. Du, H.V.R. Dias, Heterocycles 60 (2003) 1–7.
[69] L.-J. Yang, W.-T. Song, Y.-H. Luo, B.-W. Sun, Inorg. Nano-Metal Chem. 47 (2017) 493–499.
[70] M. Kondo, E. Shimizu, T. Horiba, H. Tanaka, Y. Fuwa, K. Nabari, K. Unoura, T. Naito, K. Maeda, F. Uchida, Chem. Lett. 32 (2003) 944–945.
[71] Y.-G. Sun, M.-Y. Guo, G. Xiong, F. Ding, L. Wang, B. Jiang, M.-C. Zhu, E.-J. Gao, F. Verpoort, J. Coord. Chem. 63 (2010) 4188–4200.
[72] W. Shuai, S. Cai, S. Zheng, Acta Crystallogr. E67 (2011) m897.
[73] J. Müller, Beilstein J. Org. Chem. 13 (2017) 2671–2681.
[74] J. Müller, Eur. J. Inorg. Chem. (2008) 3749–3763.
[75] M. McCann, R. Curran, M. Ben-Shoshan, V. McKee, A.A. Tahir, M. Devereux, K. Kavanagh, B.S. Creaven, A. Kellett, Dalton Trans. 41 (2012) 6516–6527.
[76] L. Brammer, M.D. Burgard, M.D. Eddleston, C.S. Rodger, N.P. Rath, H. Adams, CrystEngComm 4 (2002) 239–248.
[77] A. Bondi, J. Phys. Chem. 68 (1964) 441–451.
[78] H. Schmidbaur, A. Schier, Angew. Chem. Int. Ed. 54 (2015) 746–784.
[79] R. Tribolet, H. Sigel, Eur. J. Biochem. 163 (1987) 353–363.
[80] B. Jash, J. Neugebauer, J. Müller, Inorg. Chim. Acta 452 (2016) 181–187.
[81] K. Petrovec, B.J. Ravoo, J. Müller, Chem. Commun. 48 (2012) 11844–11846.